

Environmental Monitoring and Assessment

Climate change-induced variations in future extreme precipitation intensity-duration-frequency in flood-prone city of Adama, central Ethiopia

--Manuscript Draft--

Manuscript Number:	EMAS-D-21-01421R1
Full Title:	Climate change-induced variations in future extreme precipitation intensity-duration-frequency in flood-prone city of Adama, central Ethiopia
Article Type:	Original Research
Corresponding Author:	Dejene Tesema Bulti, M.Sc Ethiopian Institute of Architecture, Building Construction and City Development, Addis Ababa University, Addis Ababa, ETHIOPIA
Corresponding Author Secondary Information:	
Corresponding Author's Institution:	Ethiopian Institute of Architecture, Building Construction and City Development, Addis Ababa University,
Corresponding Author's Secondary Institution:	
First Author:	Dejene Tesema Bulti, M.Sc
First Author Secondary Information:	
Order of Authors:	Dejene Tesema Bulti, M.Sc Birhanu Girma Abebe Zelalem Biru, PhD.
Order of Authors Secondary Information:	
Funding Information:	
Abstract:	<p>The influences of climate change on the features of extreme rainfall events have become unprecedented that needs improved understanding at all levels for planning effective management strategies of the potential risks. This study aims to assess the potential influences of climate change on extreme rainfall characteristics in flood-vulnerable city of Adama. For this, daily precipitation records of 1967-2016 and projection of global circulation models (GCMs): CanESM2 and HadCM3 for 2021-2070 were disaggregated into shorter time resolutions using the Hyetos model. Gumbel Type I probability distribution and power-regression model ($Y = aX^b$) were used for deducing intensity-duration-frequency (IDF) curves and for describing their functions, respectively. The extreme rainfall intensity of the historical and future periods for a range of storm durations and return periods were compared and contrasted. A close agreement is obtained between the observed and the modeled rainfall intensity with high values of coefficient of determination (> 0.996) and Nash-Sutcliffe efficiency (> 0.850). Besides, statistically significant ($p < 0.05$) direct linear relationship is found between the return periods and the coefficient parameter of the IDF models. Moreover, the intensity of extreme precipitation over 2021-2070 in Adama city would increase up to 49.5%, depending on storm duration and return period considered. This could have consequences of the way the city's drainage infrastructures are designed, operated and sustained. Hence, flood-prone areas should be recognized in order to formulate effective strategies for mitigation and adaption of potential impacts. The standards for designing future drainage infrastructures should also be updated aiming to reflect the effects of climatic change. The standards for designing future drainage infrastructures should also be updated aiming to reflect the effects of climatic change.</p>
Response to Reviewers:	<p>Dear,</p> <p>The authors very much appreciate the time and dedication spent on reviewing our work. All of your remarks have significantly contributed to improving the material in one way or another.</p>

We have addressed all the comments of the reviewer 3 and our point by point response is included in "Response to reviewers.docx" file.

Regards,

[Click here to view linked References](#)

1 **Climate change-induced variations in future extreme precipitation intensity-**
2 **duration-frequency in flood-prone city of Adama, central Ethiopia**

3
4 **Dejene Tesema Bulti** ^{1*}

5 Ethiopian Institute of Architecture, Building Construction, and City Development, Addis Ababa
6 University, Addis Ababa, Ethiopia

7 E-mail: dejenetesema@yahoo.com

8 Tel: +251-930-070802

9

10 **Birhanu Girma Abebe**¹

11 Ethiopian Institute of Architecture, Building Construction, and City Development, Addis Ababa
12 University, Addis Ababa, Ethiopia

13 E-mail: birhanu.girma@eiabc.edu.et

14 Tel: +251-911-193882

15

16 **Zelalem Biru**²

17 Adama Science and Technology University, Adama, Ethiopia

18 E-mail: zelalembgd016@gmail.com

19 Tel: +251-938-107127

20

21 **Abstract**

22 The influences of climate change on the features of extreme rainfall events have become
23 unprecedented that needs improved understanding at all levels for planning effective management
24 strategies of the potential risks. This study aims to assess the potential influences of climate change
25 on extreme rainfall characteristics in flood-vulnerable city of Adama. Daily precipitation records
26 of 1967-2016 and projection of global circulation models (GCMs): CanESM2 and HadCM3 for
27 2021-2070 were disaggregated into shorter time resolutions using the Hyetos model. Gumbel Type
28 I probability distribution and power-regression model ($i = aD^b$) were used for deducing intensity-
29 duration-frequency (IDF) curves and for describing their functions, respectively. The extreme
30 rainfall intensity of the historical and future periods for a range of storm durations and return
31 periods were compared and contrasted. A close agreement is obtained between the observed and
32 the modeled rainfall intensity with high values of coefficient of determination (> 0.996) and Nash-

* Correspondence: dejenetesema@yahoo.com

33 Sutcliffe efficiency (> 0.850). Besides, statistically significant ($p < 0.05$) direct linear relationship
34 is found between the return periods and the coefficient parameter of the IDF models. Moreover,
35 the intensity of extreme precipitation over 2021-2070 in Adama city would increase up to 49.5%,
36 depending on storm duration and return period considered. This could have consequences of the
37 way the city's drainage infrastructures are designed, operated and sustained. Hence, flood-prone
38 areas should be recognized in order to formulate effective strategies for mitigation and adaption of
39 potential impacts. **The standards for designing future drainage infrastructures should also be
40 updated aiming to reflect the effects of climatic change.**

41 **Keywords:** Climate change, Precipitation intensity, Climate extreme, Flood hazard

42

43 **Funding**

44 No funding was received.

45 **Competing interests**

46 The authors declare that they have no competing interests.

47 **Availability of data and material**

48 Not applicable.

49 **Authors' contributions**

50 **Dejene Tesema Bulti:** conceptualization, data curation, methodology, analysis, interpretation
51 of the results, software, visualization and writing. **Birhanu Girma Abebe** and **Zelalem Biru:**
52 supervised the study and reviewed the whole content. All authors read and approved the
53 manuscript.

54 **Ethics approval and consent to participate**

55 Not applicable.

56 **Consent for publication**

57 We have agreed to submit to Environmental Monitoring and Assessment journal and approved
58 the manuscript for submission.

59

60 **1 Introduction**

61 Weather and climate extremes have been considered as the underlying causes of environmental
62 hazards, such as floods and landslides (Deb et al., 2018; Natarajan and Radhakrishnan, 2019;
63 Stephenson et al., 2016; Zahiri et al., 2016; Zeder and Fischer, 2020). Studies have shown the
64 potential rise in extreme precipitation events in the future period due to changes in global climate,
65 with substantial impacts on lives and properties (Barbero et al., 2019; Dastagir, 2015; Hay et al.,
66 2016; Lestari et al., 2019; Rao and Ramana, 2015; Shahid et al. 2015). Climate change influences
67 the relationship between intensity, duration and frequency (IDF) of extremes (Buba et al., 2017;
68 Fadhel et al., 2017; Yilmaz et al., 2014; Mirhosseini et al. 2012). The changes in IDF relationships
69 would have key consequences of the way the current and future urban drainage system is designed,
70 operated and sustained (Cook et al., 2020; Gebru, 2020; Moujahid et al., 2018; Sillmann et al.,
71 2017). Therefore, an enhanced understanding of the potential changes in the relationship between
72 the features of extreme rainfall events, under the changing climate has a primary importance of
73 planning sustainable urban stormwater management strategies.

74 Establishing relationship between extreme precipitation IDF for applications for urban settings
75 demands high temporal resolution of precipitation; e.g., sub-daily (Alam and Elshorbagy, 2015;
76 Courty et al., 2019; Noor et al., 2021). In developing countries like Ethiopia, however the quantity
77 and distribution of instruments capable of recording rainfall on shorter temporal scale is limited
78 (Alem et al., 2019; Beyene et al., 2019; Engida and Esteves, 2011). In response to such limitations,
79 various models, such as Hyetos, MuDRain, artificial neural network and cascade model have been
80 developed to downscale daily precipitation to a finer temporal scale and have been applied for
81 various studies (Garbrecht et al., 2017; Hanaish et al., 2011; Müller-Thomy et al., 2018; Noor et
82 al., 2018; Pui et al., 2012; Saad et al., 2018; Shrestha et al., 2017).

83 In most urban areas of Ethiopia, IDF curves provided by the Ethiopian Road Authority (ERA)
84 are used as standards for designing stormwater management infrastructures. ERA categorized the
85 country into eight rainfall regions and established IDF curves for the regions with storm length of
86 1-hr to 3-hr and six return periods (2, 5, 10, 25, 50 and 100-yr). The country is highly vulnerable
87 to variability of extreme rainfall, especially in smaller spatial scales (Beyene et al., 2019; Dawit et
88 al., 2019; Geremew et al., 2020; Mekonen and Berlie, 2019; Mohammed et al., 2018), and thus,
89 the ERA's IDF curves could overestimate or underestimate the extreme hourly rainfall magnitude
90 to some degree, when it comes to local applications. Moreover, the curves can only be used on the
91 basis of time-invariant distribution (i.e., Stationary assumption). In other words, it assumes that
92 significant changes in the extreme rainfall characteristics (e.g., Severity and frequency) overtime
93 are less likely. Such assumption, however may not be valid under the conditions of potential global
94 climate change that may result in changes in the frequency and intensity of extreme rainfall (Cheng
95 et al., 2014; Katz, 2013; Tesfay and Quraishi, 2017).

96 In this regard, few studies (Gebreigziabher, 2020; Gebremedhin, 2017; Gebru, 2020; Tesfay
97 and Quraishi, 2017) have been conducted to establish the relationships between rainfall IDF using
98 the observed and projected daily precipitation of different areas of the country. They documented
99 the IDF relationship of extreme rainfall in the present-day climate condition likely to change over
100 the future period, with different magnitude and direction for analysis areas. However, research
101 focusing on the impacts of climate change on the relationship of extreme precipitation for Adama
102 City (Regional City) is scarce. It is the fast-growing city with the population growth rate of 9%
103 from 2004 to 2016 (Bulti and Assefa, 2019). The city is highly vulnerable to urban flood (Bulti et
104 al., 2017). Hence, the results of climate change impact study in Adama City can support the efforts
105 being made to ensure sustainable development of the city.

106 The authors of the present study, recently published a research (Bulti et al., 2020) which
107 analyzed the trend of extreme rainfall in Adama city during 1965-2016 using 10 indices. By
108 downscaling daily precipitation from the Global Circulation Models (GCM) estimates for the
109 future 2021-2080, the study also assessed the potential changes in extreme precipitation events
110 based on the changes in annual percentage of wet-days, longest wet-spell, annual total
111 precipitation, and the ratio of 95th percentile and the total annual precipitation.

112 The study documented significant increasing trend of extreme precipitation in Adama city
113 over the last 52 years, and would continue to increase up to 2080. Despite the study provided a
114 valuable information about the climate change impacts on the historical and future extreme
115 precipitation events in Adama city, the relations between the features of extreme precipitation (i.e.,
116 IDF) are not well addressed. Improved understanding on the potential changes in extreme
117 precipitation characteristics due to climate change is useful for planning effective management
118 strategies of the potential risks and for designing climate-resilient urban drainage infrastructures.

119 Therefore, this study aims to expand the prior work (Bulti et al., 2020) by assessing the
120 potential influences of climate change on extreme precipitation intensity in Adama city.
121 Specifically, the study is conducted (a) to downscale daily precipitation observed during 1967-
122 2016 and GCMs projection for 2021-2070 into shorter time scales; (b) to establish rainfall IDF
123 relationships of the historical and future climate conditions; (c) to use the developed IDF models
124 and assess the possible changes in the future extreme rainfall intensity as compared to the historical
125 condition for a range of storm durations and return periods.

126 2 Materials and Methods

127 2.1 Study area

128 Adama city is located at 39° 16' E longitude and 8° 33' N latitude. The city is suited in the Rift
129 Valley, with its flat terrain features, surrounded by mountains and rugged topography. Pluvial
130 flood is almost a frequent feature of Adama City during the rainy season, causing a significant
131 damage to life and property (Bulti et al., 2017). The floodplain area is densely populated and is
132 marked by massive urban development. Fig. 1 shows the study area along with the nearby
133 metrological stations. The findings of recent studies (e.g., Mohammed et al., 2018; Mekonen
134 and Berlie, 2019; Geremew et al., 2020) indicate that the trend of long-term rainfall extreme is not
135 uniform when it comes to smaller scale local scale and suggesting a small-scale analysis is
136 essential to effectively address risks associated with climate. Hence, similar to Bulti et al. (2020),
137 Adama meteorological station was considered as a representative station for the study area. The
138 station is located at 8.55-degree latitude and 39.28-degree longitude with an altitude of 1622 m.

139 **Fig. 1** Location map of the study area, a) Regions of Ethiopia; b) Oromia Region; and c) Adama City with
140 surrounding weather observation stations

141

142 2.2 Data used

143 Two rainfall datasets were used in this study. Daily precipitation records of 1967-2016 were
144 used for establishing IDF relationship of the historical extreme rainfall. Future daily rainfall data
145 which have been spatially downscaled from the outputs of HadCM3 and CanESM2 in previous
146 research (Bulti et al., 2020) were used for establishing IDF relationship of the future period. In this
147 regard, an average of the daily rainfall data projected under the scenarios of CanESM2 (RCP2.6,

148 RCP4.5 and RCP8.5) and HadCM3 (A2a and B2a) were considered. Future 50 years (2021-2070)
149 spanned time-series were used to ensure the consistency of time-series lengths between the base
150 period and future period.

151 2.3 Methods

152 2.3.1 Derivation of sub-daily precipitation and annual maximum series

153 Precipitation data of both the present and future periods were limited to a daily time resolution.
154 In order to extract annual maximum precipitation at sub-daily resolution, the daily rainfall depths
155 were disaggregated into hourly values using a Hyetos computer program. It is an easy temporal
156 downscaling software, and freely available at <http://www.itia.ntua.gr/e/softinfo/3/>. Hyetos has
157 been used in a number of studies in different regions of the world (Beyene et al., 2019; Engida and
158 Esteves, 2011; Kossieris and Efstratiadis, 2015; Shrestha et al., 2017). Hyetos uses the Bartlett–
159 Lewis model (BLM) and the adjustment procedures for the disaggregation process. The description
160 of the model and the meaning of its parameters can be found elsewhere (Sun et al., 2019).

161 In response to the existing limited hourly rainfall records to be used for the disaggregation
162 model calibration, validated BLM parameter values (Table 1) for the Addis Ababa station were
163 adopted from (Beyene et al., 2019). It is the nearest station to the study area, among the stations
164 with validated values available. In addition, both Addis Ababa and Adama stations are located
165 within the upper Awash basin (Shawul and Chakma, 2020), and rainfall Regime-A which covers
166 the central part of the country with the bimodal rainfall system (Berhanu et al., 2014). Using hourly
167 data, thus obtained, rainfall depths for larger time-windows (3-hr, 6-hr and 12-hr) was generated.
168 Finally, the sets of annual maximum (AMAX) corresponding to five storm durations (1-hr, 3-hr,
169 6-hr, 12-hr and 24-hr) for the analysis periods, 1967-2016 and 2021-2070, were extracted.

170

171 **Table 1** Values of BLM parameters used in disaggregation process, adopted from (Beyene et al.,
172 2019)

173

174 Using the AMAX datasets, descriptive statistical analysis was conducted on the basis of
175 skewness. The skewness index describes the shape of the distribution. It takes the value zero for a
176 symmetrical distribution. However, a skewness of exactly zero is quite unlikely to real-world data.
177 In this study, the skewness values between -2 and +2 were considered for normal distribution
178 (Muzaffar, 2016). Values less than -2 and greater than +2 indicate negatively skewed and
179 positively skewed distribution, respectively. This helped to provide an overview of the data series
180 used in the study.

181 **2.3.2 Developing IDF relationship**

182 The modeling of the rainfall IDF relationships involves a series of steps that can be categorized
183 as determining probable maximum rainfall; estimating rainfall intensity; determining the fitting
184 model parameters; and assessing the model performance of the fitting model (validation). In
185 addition, correlation between return periods and model fitting parameters was assessed.

186 *Estimation of probable maximum precipitation (PMP):* It is the extreme rainfall depth for a
187 defined period, which is meteorologically possible for a given watershed at a given time of year,
188 without taking into account long-term climate trends. PMP is usually determined by fitting annual
189 maximum rainfall series to a suitable theoretical probability distribution. Gumbel's extreme value
190 distribution type I (EVI) was employed to fit each set of annual maximum rainfall series
191 corresponding to five time-windows (1-hr, 3-hr, 6-hr, 12-hr, and 24-hr) for eight return periods (5-

192 yr, 10-yr, 25-yr, 50-yr, 100-yr, 300-yr, 500-yr and 1000-yr). EVI is the agreed probability
 193 distribution for meteorological and hydrological studies (Bhagat, 2017; Bharali, 2015; Coronado-
 194 Hernández et al., 2020; de Paola et al., 2014; Gebremedhin, 2017; Gebru, 2020; Tesfay and
 195 Quraishi, 2017). In this case, for respective storm duration and recurrence interval, PMP was
 196 computed using Equation 1.

$$197 \quad PMP_{T_d} = \bar{X}_d + K_T S_d \quad \dots (1)$$

198 Where: \bar{X}_d and S_d are the mean and the standard deviation of each set of annual maximum
 199 precipitation series (function of storm duration), respectively, and K_T is a frequency factor
 200 depending on the return period (T), and calculated using Equation 2 (Mujere, 2011).

$$201 \quad K_T = -\frac{\sqrt{6}}{\pi} \left[0.5772 + \ln \left(\ln \left(\frac{T}{T-1} \right) \right) \right] \quad \dots (2)$$

202
 203
 204 *Estimation of intensity:* Using the values of PMP, the rainfall intensity was determined as the
 205 average precipitation depth that falls per time increment, and measured in millimeter per hour (de
 206 Paola et al., 2014; Tesfay and Quraishi, 2017). Accordingly, the rainfall intensity was computed
 207 by dividing probable maximum precipitation for the corresponding storm duration (Equation 3).
 208 This helped to identify the relationships of the features of extreme rainfall (intensity, duration and
 209 return period). The relations were checked for self-similarity (Erena et al., 2018a); i.e., they are
 210 assumed to have a consistent pattern for each return period.

$$211 \quad I_d = \frac{PMP_{T_d}}{d} \quad \dots (3)$$

212 Where: $PMP_{T,d}$ probable maximum precipitation (mm) corresponding to a T-year event for
 213 the d -rainfall duration, and d is storm duration (hour).

214 *Deriving IDF model equations:* the empirical equations (mathematical models) used to
 215 describe the IDF relationships were derived using bi-parameter power-regression model. For each
 216 return period, a functional relationship between the corresponding extreme rainfall intensity and
 217 the storm duration can be expressed as Equation 4 (de Paola et al., 2014). In this case, values of
 218 fitting parameters (i.e., $a(T)$ and b) are regressed for each return period, and they were calculated
 219 by Equations 5 and 6.

$$220 \quad I(d, T) = a(T)d^b \quad \dots (4)$$

$$221 \quad b = \frac{n \sum_{i=1}^n (\ln x_i \ln y_i) - \sum_{i=1}^n (\ln x_i) \sum_{i=1}^n (\ln y_i)}{n \sum_{i=1}^n (\ln x_i)^2 - (\sum_{i=1}^n \ln x_i)^2} \quad \dots (5)$$

$$222 \quad a(T) = e^{\left(\frac{\sum_{i=1}^n (\ln y_i) - b \sum_{i=1}^n (\ln x_i)}{n} \right)} \quad \dots (6)$$

223
 224
 225 Where: $a(T)$ and b are the regression parameters, n is the number of number of storm durations
 226 (time-windows) considered, x_i and y_i are storm durations (hour) and corresponding intensity
 227 (mm/hr.), respectively.

228 *Model validation:* the model of IDF relationship was validated using graphical and statistical
 229 method. First, the self-similarity of n values was checked for each return period; i.e., uniform
 230 pattern is expected (Erena and Worku, 2018). Second, the goodness-of-fit of the mathematical
 231 models was assessed using two statistical parameters: coefficient of determination (R^2) and Nash-
 232 Sutcliffe efficiency (NSE), which were determined using Equations 7 and 8, respectively. The

233 value of R^2 ranges -1 to 1 and that of NSE can vary from $-\infty$ to 1. The optimum value of the two
 234 chosen parameters is 1, indicating the perfect fit of the derived model to the data (Lacombe et al.,
 235 2014; Waseem et al., 2017). In this study, the minimum criteria recommended by (Moriassi et al.,
 236 2007) for both parameters ($NSE > 0.5$ and $R^2 > 0.7$) were adopted. The model is considered valid
 237 only if it satisfies these criteria at a time.

$$238 \quad R^2 = \left[\frac{\sum_{i=1}^n (x_{O_i} - \bar{x}_O)(x_{P_i} - \bar{x}_P)}{\sqrt{\sum_{i=1}^n (x_{O_i} - \bar{x}_O)^2} \sqrt{\sum_{i=1}^n (x_{P_i} - \bar{x}_P)^2}} \right]^2 \quad \dots (7)$$

$$239 \quad NSE = 1 - \frac{\sum_{i=1}^n (x_{O_i} - x_{P_i})^2}{\sum_{i=1}^n (x_{O_i} - \bar{x}_O)^2} \quad \dots (8)$$

240 Where: x_O and x_P are observed (used for calibration) and simulated (computed using IDF
 241 equations) rainfall intensities, respectively; and \bar{x}_O and \bar{x}_P are the corresponding mean
 242 values

243
 244 *Correlation analysis:* It was carried to assess the extent to which the power-law fitting
 245 parameters are linear related to the return period. It was determined based on value of Pearson's
 246 correlation coefficient (r) computed using return periods and the values of both parameters in the
 247 validated IDF models. The strength of the relationship was described using the absolute value of
 248 correlation coefficient: very weak ($|r| < 0.19$), weak ($|r| < 0.39$), moderate ($|r| < 0.59$), strong ($|r| <$
 249 0.79), very strong ($|r| < 1$). Moreover, the statistical significance of the relationships was assessed
 250 based on p-value statistics at 95% confidence level ($p < 0.05$).

251 2.2.3 Analysis of changes in precipitation intensity

252 The potential changes in extreme precipitation intensity were assessed in two ways. First, the
253 changes in intensity were assessed using graphical comparison by overlaying the IDF curves of
254 historical and future periods. Second, the magnitude of changes was determined in terms of relative
255 percentage difference between the intensity of corresponding storm durations and return periods.
256 For this reason, the extreme precipitation intensity for a range of storm durations and return periods
257 were calculated using the IDF models developed in this study. The percentage of relative
258 differences were then determined using Equation 8, a widely used approach in most climate change
259 studies (Gebru, 2020; Solaiman and Simonovic, 2011; Tesfay and Quraishi, 2017).

260

$$261 \quad \text{Relative difference (\%)} = \frac{x_F - x_H}{\frac{1}{2}(x_F + x_H)} * 100 \quad \dots (8)$$

262 Where: x_F and x_H are extreme rainfall intensities computed based on the future and the
263 historical IDF relationships, respectively.

264

265 3 Results

266 3.1 Annual maximum precipitation series

267 Daily rainfall data recorded during 1967-2016 and predicted for the future 2021-2070 under
268 two GCMs were disaggregated into shorter time scales. AMAX rainfall series of storm durations
269 1-hr, 3-hr, 6-hr, 12-hr and 24-hr was extracted for respective analysis timelines. Skewness index
270 was computed for each dataset. The computed values of skewness are summarized in Table 2, and
271 provides information about the shape of the distribution of the datasets. In all the cases, the values

272 are found to be positive and less than 2.0; i.e., within the criteria considered for normal distribution
273 ($-2 < \text{skewness} < +2$). The AMAX sub-daily rainfall series obtained through disaggregation process
274 has similar distribution, with that of the corresponding daily precipitation.

275

276 **Table 2** Skewness of AMAX daily and sub-daily rainfall series during the past and future timelines

277

278 **3.2 Rainfall IDF relationships**

279 **3.2.1 IDF curves**

280 Fig. 2 illustrates the IDF curves of extreme rainfall in Adama city for the periods 1967-2016,
281 historical (a), HadCM3 (b) CanESM2 (c). They are developed by fitting GEV I to the respective
282 AMAX precipitation series. The curves give information about the magnitude of rainfall intensity
283 as a function of storm durations from 1-hr to 24-hr and return periods from 5-yr to 300-yr.

284 The IDF curves clearly show that rainfall intensity decreases, as duration of the storm
285 increases from 1-hr to 24-hr. For storms from 1-hr to 24-hr, the rainfall intensity increases, as
286 return period increases from 5-yr to 300-yr. The results confirm that the pattern of the IDF curves
287 of the respective study periods satisfied self-similarity and are consistent with the expected
288 behavior of the IDF curve. Comparatively, the HadCM3 curves do not show significant difference
289 in intensity for storms longer than 12-hr.

290 **Fig. 2** Precipitation IDF curves of the past and future timelines a) historical 1967-2016, future
291 projection b) HadCM3, and c) CanESM2

292

293

294 3.2.2 IDF models

295 Results summarized in Table 3 show the mathematical equations of respective IDF models
296 alongside the computed values of coefficient of determination and Nash-Sutcliffe efficiency. From
297 the equations of the respective IDF models, it is evident that the value of coefficient parameter
298 increases, as frequency decreases from more frequent (5-yr) to less frequent (300-yr) storms, in all
299 datasets. Similarly, the value (absolute) of exponent parameter increases, with return period for
300 the historical and HadCM3 datasets and on the contrary of CanESM2.

301 **Table 3** Summary of the IDF model equations for the present and future rainfall in Adama city (*d*:
302 rainfall duration (hour)) and the corresponding results of model performance evaluation (R^2 :
303 Coefficient of determination, *NSE*: Nash-Sutcliffe efficiency)

304

305 With regard to the results of model performance evaluation, high values are obtained for the
306 selected statistical parameters. The computed value of coefficient of determination ranges 0.996 –
307 1.0 and that of Nash-Sutcliffe efficiency is between 0.584 and 0.998, for the analysis periods and
308 datasets considered in this study. The results greater than the threshold considered for both
309 parameters in this study ($NSE > 0.5$ and $R^2 > 0.7$), and satisfied all considered model performance
310 evaluation criteria at a time.

311 3.3.3 Relationship of return periods and IDF model parameters

312 The extent of the relationship between return period and the individual model parameters (i.e.,
313 coefficient and exponent parameters) was also assessed using correlation analysis. The computed
314 correlation coefficient and the p-value are shown in Table 4. The results show that the fitting
315 parameters of IDF models are positively correlated with the return periods. The observed

316 relationships are found to be very strong (i.e., $r > 0.79$) for most of the cases and strong ($r > 0.59$)
317 for exponent parameter in the case of historical and CanESM2.

318 Moreover, the significance test of the linear relationship of coefficient parameter with return
319 periods resulted in the p-value smaller than 0.05 in all of the cases, indicates the relationship is
320 statistically significant. On the other hand, the p-value is found to be greater than 0.05 for the case
321 of exponent parameter, indicates the observed linear relationship is not significant, at the selected
322 analysis level.

323 **Table 4** Results of correlation analysis between fitting parameters power-law function ($i = aD^b$)
324 and return periods

325

326 **3.3 Future changes in rainfall intensity**

327 The potential changes in extreme precipitation intensity in the future period as compared to the
328 baseline period were assessed based on the two GCMs. Fig. 3 compares the historical IDF curves
329 with that of future period based on the selected GCMs, HadCM3 and CanESM2. Table 5 also
330 provides information about the magnitude and direction of changes in the future extreme rainfall
331 intensity relative to that of the baseline climate condition at 1-hr, 3-hr, 6-hr, 12-hr and 24-hr rainfall
332 durations and all return periods considered in this study.

333 **Fig. 3** Comparison of historical IDF curves (1967-2016) with Projected IDF curves (2021-2070)

334 **Table 5** Percentage change of future intensity relative to historical condition (T: return period
335 (year), d: storm duration (hour))

336 Overall, the IDF curves demonstrate that the rainfall intensity over the future period will be
337 different from the baseline period. In all the cases, the HadCM3 curves show smaller intensity than

338 that of historical and CanESM2. Except for 5-yr return period, IDF curves corresponding to
339 CanESM2 GCM show that intensity of the extreme rainfall will be higher, for longer storms and
340 will be lower for shorter storms than the baseline condition. In this regard, extreme rainfall events
341 with 15-hr, 7-hr, 5-hr, 4-hr and 3-hr storm durations corresponding to return periods 10-yr, 25-yr,
342 50-yr, 100-yr and 300-yr, respectively, will approximately reproduce historical rainfall intensity.
343 However, IDF curves HadCM3 show less intensified rainfall than that of the baseline period under
344 all storm durations and return periods. The decreasing magnitude is maximum for the shortest
345 storm (1-hr), despite the value is found to decline towards the longest storm (24-hr).

346 Turning to the results summarized in Table 5, rainfall intensity in Adama city will change in
347 the future by significant percentage relative to that of the baseline period. In addition, significant
348 difference can be seen in the identified changes by the GCMs. With regard to HadCM3 projection,
349 future rainfall intensity will decrease by significant percentage, for all storm durations and return
350 periods. The magnitude of percentage changes is also found to increase from more frequent rainfall
351 of shorter duration (1-hr 5-yr) to less frequent rainfall of longer duration (24-hr 300-yr).
352 Conversely, results based on CanESM2 projections reveal that the magnitude of decreasing change
353 in intensity predicted by CanESM2 GCM declines and that of increasing changes increases, with
354 return periods and respective storm durations. It is also evident that HadCM3 predicted the relative
355 decrease future daily rainfall intensity ranges 87.5%(T=5-yr)-106.2%(T=300-yr). With similar
356 length of storm (24-hr), CanESM2 predicted 13.3% decrease corresponding to 5-yr return period
357 and an increase in intensity by 9.1% (T=10-yr)-49.5% (T=300-yr).

358

359 4 Discussion

360 The changes in the characteristics of extreme rainfall due to global climate change have
361 contributed to the increased rainfall-induced urban flooding in most parts of the world. Adama city
362 is among flood-vulnerable urban settings in Ethiopia. An improved understanding of how the
363 characteristics of extreme rainfall do change due to climate change, at a local scale is imperative
364 for planning effective management strategies of the potential risks. By disaggregating daily rainfall
365 records and future projections of GCMs, the IDF models were developed, and applied for
366 examining the extent to which the present-day extreme rainfall intensity will be reproduced under
367 future climate condition.

368 In the process of fitting bi-parametric power-law function ($i = a D^b$) to the data, high values
369 are obtained for coefficient of determination in all the cases and for Nash-Sutcliffe efficiency in
370 most of the cases, indicate a good agreement of the observed (i.e., computed from rainfall depths)
371 and simulated rainfall intensity using the developed IDF models. The results are comparable with
372 that of similar studies (Erena et al., 2018b; Ewea et al., 2018; Gebru, 2020), and confirm a good
373 performance of the IDF models in explaining the relationship between intensity, duration and
374 frequency of extreme precipitation in Adama city under the study's conditions (i. e., datasets, storm
375 durations, return periods and analysis timelines). In addition, the findings reflect the successful
376 application of Gumbel's type I probability distribution and the bi-parametric power-regression
377 function, for constructing IDF curves and for deriving the equations of the models, respectively.

378 Statistically significant direct linear relationship is obtained between the values of coefficient
379 parameter (i.e., parameter a) and the corresponding return periods, in all models developed using
380 the observed and projected rainfall datasets and on the contrary for exponent parameter (i.e.,

381 parameter b). This finding is consistent with the findings of (Ewea et al., 2018) who modeled IDF
382 curves in Makkah Al Mukarramah region for designing stormwater infrastructures.

383 Moreover, the findings reveal that the extreme rainfall intensity in the future period in Adama
384 city would rise or decline, depending on GCM, storm duration and return period considered. Under
385 the projection of CanESM2, the intensity of shorter storms will decrease and that of longer storms
386 increase, under all return periods greater than 5-yr. The results based on HadCM3 prediction reveal
387 that the intensity of future extreme precipitation will decrease more than by half of its historical
388 value, in all the cases. In accordance with these findings, studies have documented mixed results,
389 decreasing and increasing, of changes in extreme rainfall intensity due to climate change in
390 different areas of the country, including Mekele city (Gebreigziabher, 2020), some parts of Tigray
391 region (Gebru, 2020) and Chiro and Hurso (Tesfay and Quraishi, 2017). The findings of the
392 present study are pertaining to Adama city which has received little attention. The significant
393 differences between the results of the GCMs used in this study could be associated with
394 uncertainties in the GCMs in predicting rainfall pattern (Noor et al., 2018), and highlight the results
395 of climate change impacts studies could be affected by our choice of GCMs for future climate
396 projections. For planning of mitigation and adaption measures, it is ideal to consider the variations
397 under the increasing scenario.

398 Considering the findings, it is reasonable to conclude that extreme rainfall intensity over the
399 coming 50 years (2021-2070) in Adama city likely to change due to climate change. An increase
400 rainfall intensity could have an impact on the conveyance capacity of the existing stormwater
401 drainage system, and could result more frequent and severe floods than in the past years. Moreover,
402 the current practice of stormwater infrastructure design based on the assumption of time-invariant

403 rainfall distribution may not provide reliable result to maintain the future potential increase in
404 extreme rainfall due to climate change.

405 With respect to the increasing concern of management of climate change-induced urban
406 flooding in general and in Adama city in particular, the significance of this study can be explained
407 in different ways. The potential changes in extreme rainfall intensity identified here contribute to
408 a clear understanding of the effects of climate change on the future extreme precipitation
409 characteristics, and support local climate change adaption planning as well as decision-making.
410 The findings can also be used in revision of the current regulations and standards for the planning
411 and designing of urban drainage systems at local level. Moreover, they have paramount importance
412 of future studies, particularly the assessment of flood hazard and risk of the City under the effects
413 of changes in global climate in order to formulate effective flood mitigation and adaption
414 strategies.

415 In urban settings, reliably established relationships between features of extreme rainfall has a
416 primary importance of designing a new stormwater infrastructures and assessing the potential risk
417 of existing drainage system. The IDF models developed in this study enable to estimate extreme
418 precipitation intensity for a wider range of storm durations and for a number of return periods; i.e.,
419 from more frequent rainfall of shorter duration (1-hr 5-yr) to less frequent rainfall of longer
420 duration (24-hr 300-yr) over different analysis periods. IDF models of more-frequent shorter
421 durations can be used for stormwater management applications and a less-frequent longer-duration
422 events are useful for flood risk management in the City under future climate conditions. Moreover,
423 mathematical equations of the rainfall IDF relationships can reduce the dependency on the
424 graphical versions of the models and allow to better determine any of the three features of the

425 storm (intensity, duration, frequency) using the other two attributes, at specific duration from 1-hr
426 to 24-hr.

427 On top of satisfying the objectives of this study, the findings build on existing evidences and
428 offers valuable insights into the influences of climate change on extreme precipitation; the
429 uncertainties of GCMs in the predicting precipitation characteristics; the relationships between
430 return period and fitting parameters of the power-law function and the potential application of
431 methodology used in the present study.

432 **5 Conclusions**

433 The intent of this study was to provide information about the potential influences of climate
434 change on IDF of extreme rainfall in Adama city. For this, daily precipitation records of 1967-
435 2016 and projected for 2021-2070 periods were disaggregated into shorter time scale, and used for
436 developing rainfall IDF models. By computing rainfall intensity for a range of storm durations and
437 return periods using the models, the percentage change of future rainfall intensity relative to the
438 current climate condition was determined.

439 A close agreement is obtained between the observed and the modeled rainfall intensity with
440 high values of coefficient of determination and Nash-Sutcliffe efficiency. Besides, statistically
441 significant ($p < 0.05$) direct linear relationship is found between return periods and coefficient
442 parameter of IDF models. Moreover, the intensity of extreme precipitation over the years 2021-
443 2070 in Adama city would be different from the historical condition, depending on GCM, storm
444 duration and return period considered. For storm duration (24-hr), the maximum increase is 49.5%
445 (CanESM2) and decrease up to 106.2% (HadCM3).

446

447 This study suggests the characteristics of extreme rainfall in Adama city over the coming 50
448 years likely to change due to global climate change. This could have consequences of the way the
449 city's drainage infrastructures are designed, operated and sustained. The city has experienced
450 devastating rainfall-induced flood events in the past and could experience more frequent and
451 severe floods in the future due to the possible rise in extreme precipitation intensity under changing
452 climate. Hence, future research is needed to assess the potential flood hazard under changing
453 climate in order to formulate effective mitigation and adaption strategies for the associated risks.
454 Moreover, the standards and guidelines presently employed by the city for the design of
455 stormwater management infrastructure should be revised in order to reflect the global climate
456 change impacts.

457 **Acknowledgements**

458 This paper is a part of ongoing PhD dissertation by Dejene Tesema Bulti at Ethiopian Institute
459 of Architecture, Building Construction and City Development (EiABC), Addis Ababa University,
460 Ethiopia.

461

462

463 **6 References**

464 Alam, S., Elshorbagy, A., 2015. Quantification of the climate change-induced variations in
465 Intensity – Duration – Frequency curves in the Canadian Prairies. JOURNAL OF
466 HYDROLOGY 527, 990–1005. <https://doi.org/10.1016/j.jhydrol.2015.05.059>

467 Alem, A.M., Tilahun, S.A., Moges, M.A., Melesse, A.M., 2019. A regional hourly maximum
468 rainfall extraction method for part of Upper Blue Nile Basin, Ethiopia, in: Extreme
469 Hydrology and Climate Variability. Elsevier Inc., pp. 93–102.
470 <https://doi.org/10.1016/B978-0-12-815998-9.00009-9>

471 Barbero, R., Fowler, H.J., Blenkinsop, S., Westra, S., Moron, V., Lewis, E., Chan, S., Lenderink,
472 G., Kendon, E., Guerreiro, S., Li, X.F., Villalobos, R., Ali, H., Mishra, V., 2019. A
473 synthesis of hourly and daily precipitation extremes in different climatic regions. *Weather*
474 and *Climate Extremes* 26. <https://doi.org/10.1016/j.wace.2019.100219>

475 Berhanu, B., Seleshi, Y., Melesse, A.M., 2014. Surface Water and Groundwater Resources of
476 Ethiopia: Potentials and Challenges of Water Resources Development. In: A. M. Melesse
477 et al. (eds.), *Nile River Basin*, pp. 97-117. https://doi.org/10.1007/978-3-319-02720-3_6

478 Beyene, T.D., Moges, M.A., Tilahun, S.A., 2019. Development of rainfall disaggregation model
479 in the Awash River Basin, Ethiopia, in: *Advances of Science and Technology 6th EAI*
480 *International Conference, ICAST 2018*. Springer International Publishing, pp. 50–64.
481 https://doi.org/10.1007/978-3-030-15357-1_4

482 Bhagat, N., 2017. Flood Frequency Analysis Using Gumbel's Distribution Method: A Case
483 Study of Lower Mahi Basin, India. *Journal of Water Resources and Ocean Science* 6, 51–
484 54. <https://doi.org/10.11648/j.wros.20170604.11>

485 Bharali, B., 2015. A Study on Frequency Analysis for Puthimari Catchment by Gumbel
486 Distribution Method. *Journal of Civil Engineering and Environmental Technology* 2, 19–
487 22.

488 Buba, L.F., Kura, N.U., Dakagan, J.B., 2017. Spatiotemporal trend analysis of changing rainfall
489 characteristics in Guinea Savanna of Nigeria. *Modeling Earth Systems and Environment*.
490 <https://doi.org/10.1007/s40808-017-0356-2>

491 Bulti, D.T., Abebe, B.G., Biru, Z., 2020. Analysis of the changes in historical and future extreme
492 precipitation under climate change in Adama city, Ethiopia. *Modeling Earth Systems and*
493 *Environment*. <https://doi.org/10.1007/s40808-020-01019-x>

494 Bulti, D.T., Assefa, T., 2019. Analyzing ecological footprint of residential building construction
495 in Adama City, Ethiopia. *Environmental Systems Research* 8.
496 <https://doi.org/10.1186/s40068-019-0130-8>

497 Bulti, D. T., Mekonnen, B., Bekele, M., 2017. Assessment of Adama City Flood Risk Using
498 Multicriteria Approach. *The Ethiopian Journal of Science and Sustainable Development*
499 (EJSSD) 4(1), 6-23

500 Cheng, L., AghaKouchak, A., Gilleland, E., Katz, R.W., 2014. Non-stationary extreme value
501 analysis in a changing climate. *Climatic Change*. [https://doi.org/10.1007/s10584-014-](https://doi.org/10.1007/s10584-014-1254-5)
502 1254-5

503 Cook, L.M., McGinnis, S., Samaras, C., 2020. The effect of modeling choices on updating
504 intensity-duration-frequency curves and stormwater infrastructure designs for climate
505 change. *Climatic Change* 159, 289–308. <https://doi.org/10.1007/s10584-019-02649-6>

506 Coronado-Hernández, Ó.E., Merlano-Sabalza, E., Díaz-Vergara, Z., Coronado-Hernández, J.R.,
507 2020. Selection of hydrological probability distributions for extreme rainfall events in the
508 regions of Colombia. *Water* 12. <https://doi.org/10.3390/W12051397>

509 Courty, L.G., Wilby, R.L., Hillier, J.K., Slater, L.J., 2019. Intensity-duration-frequency curves at
510 the global scale. *Environmental Research Letters* 14. [https://doi.org/10.1088/1748-](https://doi.org/10.1088/1748-9326/ab370a)
511 9326/ab370a

512 Dastagir, M.R., 2015. Modeling recent climate change induced extreme events in Bangladesh: A
513 review. *Weather and Climate Extremes* 7, 49–60.
514 <https://doi.org/10.1016/j.wace.2014.10.003>

515 Dawit, M., Halefom, A., Teshome, A., Sisay, E., Shewayirga, B., Dananto, M., 2019. Changes and
516 variability of precipitation and temperature in the Guna Tana watershed, Upper Blue Nile
517 Basin, Ethiopia. *Modeling Earth Systems and Environment*.
518 <https://doi.org/10.1007/s40808-019-00598-8>

519 de Paola, F., Giugni, M., Topa, M.E., Bucchignani, E., 2014. Intensity-Duration-Frequency (IDF)
520 rainfall curves, for data series and climate projection in African cities. *SpringerPlus* 3, 1–
521 18. <https://doi.org/10.1186/2193-1801-3-133>

522 Deb, P., Babel, M.S., Denis, A.F., 2018. Multi-GCMs approach for assessing climate change
523 impact on water resources in Thailand. *Modeling Earth Systems and Environment*.
524 <https://doi.org/10.1007/s40808-018-0428-y>

525 Engida, A.N., Esteves, M., 2011. Characterization and disaggregation of daily rainfall in the Upper
526 Blue Nile Basin in Ethiopia. *Journal of Hydrology* 399, 226–234.
527 <https://doi.org/10.1016/j.jhydrol.2011.01.001>

528 Erena, S.H., Worku, H., 2018. Flood risk analysis : causes and landscape based mitigation
529 strategies in Dire Dawa city , Ethiopia. *Geoenvironmental Disasters* 5.
530 <https://doi.org/10.1186/s40677-018-0110-8>

531 Erena, S.H., Worku, H., de Paola, F., 2018a. Flood hazard mapping using FLO-2D and local
532 management strategies of Dire Dawa city , Ethiopia *Journal of Hydrology : Regional*
533 *Studies* Flood hazard mapping using FLO-2D and local management strategies of Dire
534 Dawa city , Ethiopia. *Journal of Hydrology: Regional Studies* 19, 224–239.
535 <https://doi.org/10.1016/j.ejrh.2018.09.005>

536 Erena, S.H., Worku, H., Paola, F. De, 2018b. Flood hazard mapping using FLO-2D and local
537 management strategies of Dire Dawa city , Ethiopia *Journal of Hydrology : Regional*
538 *Studies* Flood hazard mapping using FLO-2D and local management strategies of Dire
539 Dawa city , Ethiopia. *Journal of Hydrology: Regional Studies* 19, 224–239.
540 <https://doi.org/10.1016/j.ejrh.2018.09.005>

541 Ewea, H.A., Elfeki, A.M., Bahrawi, J.A., Al-amri, N.S., 2018. Modeling of IDF curves for
542 stormwater design in Makkah Al Mukarramah region , The Kingdom of Saudi Arabia.
543 *Open Geoscience* 10, 954–969.

544 Fadhel, S., Rico-ramirez, M.A., Han, D., 2017. Uncertainty of Intensity – Duration – Frequency (
545 IDF) curves due to varied climate baseline periods. *Journal of Hydrology* 547, 600–612.
546 <https://doi.org/10.1016/j.jhydrol.2017.02.013>

547 Garbrecht, J.D., Gyawali, R., Malone, R.W., Zhang, J.C., 2017. Cascade Rainfall Disaggregation
548 Application in U.S. Central Plains. *Environment and Natural Resources Research* 7, 30–
549 43. <https://doi.org/10.5539/enrr.v7n4p30>

550 Gebreigziabher, E.T., 2020. Analysis Rainfall Intensity-Duration-Frequencyrelationships Under
551 Climate Change for Mekele City, Ethiopia. *International Journal of Technical Research &*
552 *Science* 05, 1–11. <https://doi.org/10.30780/ijtrs.v05.i02.001>

553 Gebremedhin, Y.G., 2017. Development of Rainfall Intensity-Duration-Frequency (IDF)
554 Relationships for Siti Zone , In Case of Ethiopia Somali Regional State. *Civil and*
555 *Environmental Research* 9, 10–28.

556 Gebru, T.A., 2020. Rainfall Intensity-Duration-Frequency Relations under Changing Climate for
557 Selected Stations in the Tigray Region, Ethiopia. *Journal of Hydrologic Engineering* 25.
558 [https://doi.org/10.1061/\(asce\)he.1943-5584.0001999](https://doi.org/10.1061/(asce)he.1943-5584.0001999)

559 Geremew, G.M., Mini, S., Abegaz, A., 2020. Spatiotemporal variability and trends in rainfall
560 extremes in Enebsie Sar Midir district , northwest Ethiopia. *Modeling Earth Systems and*
561 *Environment*. <https://doi.org/10.1007/s40808-020-00749-2>

562 Hanaish, I.S., Ibrahim, K., Jemain, A.A., 2011. Daily Rainfall Disaggregation Using HYETOS
563 Model for Peninsular Malaysia. *Recent Researches in Applied Mathematics, Simulation*
564 *and Modelling* 146–150.

565 Hay, J.E., Easterling, D., Ebi, K.L., Kitoh, A., Parry, M., 2016. Conclusion to the special issue:
566 Observed and projected changes in weather and climate extremes. *Weather and Climate*
567 *Extremes* 11, 103–105. <https://doi.org/10.1016/j.wace.2015.11.002>

568 Katz, R.W., 2013. Statistical Methods for Nonstationary Extremes, in: AghaKouchak, A.,
569 Easterling, D., Hsu, K., Schubert, S., Sorooshian, S. (Eds.), *Extremes in a Changing*
570 *Climate: Detection, Analysis and Uncertainty*. Springer Dordrecht Heidelberg, New York,
571 pp. 15–37. https://doi.org/10.1007/978-94-007-4479-0_2

572 Kossieris, P., Efstratiadis, A., 2015. European Geosciences Union General Assembly 2015
573 Assessing the performance of Bartlett-Lewis model on the simulation of Athens rainfall
574 Panagiotis Kossieris , Andreas Efstratiadis , Ioannis Tsoukalas School of Civil
575 Engineering. <https://doi.org/10.13140/RG.2.2.14371.25120>

576 Lacombe, G., Douangsavanh, S., Vogel, R.M., McCartney, M., Chemin, Y., Rebelo, L.M.,
577 Sotoukee, T., 2014. Multivariate power-law models for streamflow prediction in the
578 Mekong Basin. *Journal of Hydrology: Regional Studies* 2, 35–48.
579 <https://doi.org/10.1016/j.ejrh.2014.08.002>

580 Lestari, S., King, A., Vincent, C., Karoly, D., Protat, A., 2019. Seasonal dependence of rainfall
581 extremes in and around Jakarta, Indonesia. *Weather and Climate Extremes* 24.
582 <https://doi.org/10.1016/j.wace.2019.100202>

583 Mekonen, A.A., Berlie, A.B., 2019. Spatiotemporal variability and trends of rainfall and
584 temperature in the Northeastern Highlands of Ethiopia. *Modeling Earth Systems and*
585 *Environment*. <https://doi.org/10.1007/s40808-019-00678-9>

586 Mirhosseini G., Srivastava P., Stefanova L., 2013. The impact of climate change on rainfall
587 Intensity–Duration–Frequency (IDF) curves in Alabama. *Reg Environ Change* 13, S25–
588 S33. <https://doi.org/10.1007/s10113-012-0375-5>

589 Mohammed, Y., Yimer, F., Tadesse, M., Tesfaye, K., 2018. Variability and trends of rainfall
590 extreme events in north east highlands of Ethiopia. *International Journal of Hydrology*
591 *Research* 2, 594–605. <https://doi.org/10.15406/ijh.2018.02.00131>

592 Moriasi, D.N., Arnold, J.G., Liew, M.W. Van, Bingner, R.L., Harmel, R.D., Veith, T.L., 2007.
593 MODEL EVALUATION GUIDELINES FOR SYSTEMATIC QUANTIFICATION OF
594 ACCURACY IN WATERSHED SIMULATIONS. *American Society of Agricultural and*
595 *Biological Engineers* ISSN 50, 885–900.

596 Moujahid, M., Stour, L., Agoumi, A., Saidi, A., 2018. Regional approach for the analysis of annual
597 maximum daily precipitation in northern Morocco. *Weather and Climate Extremes* 21, 43–
598 51. <https://doi.org/10.1016/j.wace.2018.05.005>

599 Mujere, N., 2011. Flood Frequency Analysis Using the Gumbel Distribution. *International Journal*
600 *on Computer Science and Engineering (IJCSE)* 3, 2774–2778.

601 Müller-Thomy, H., Wallner, M., Förster, K., 2018. Rainfall disaggregation for hydrological
602 modeling: Is there a need for spatial consistence? *Hydrology and Earth System Sciences*
603 22, 5259–5280. <https://doi.org/10.5194/hess-22-5259-2018>

604 Muzaffar, M.B., 2016. The Development and Validation of a Scalte to Measure Training Culture:
605 The TC Scale. *Journal of Culture, Society and Development* 23, 49–58.

606 Natarajan, S., Radhakrishnan, N., 2019. Simulation of extreme event - based rainfall – runoff
607 process of an urban catchment area using HEC - HMS. *Modeling Earth Systems and*
608 *Environment*. <https://doi.org/10.1007/s40808-019-00644-5>

609 Noor, M., Ismail, T., Chung, E.-S., Shahid, S., Sung, J.H., 2018. Uncertainty in rainfall intensity
610 duration frequency curves of Peninsular Malaysia under changing climate scenarios. *Water*
611 10. <https://doi.org/10.3390/w10121750>

612 Noor, M., Ismail, T., Shahid, S., Dewan, A., 2021. Evaluating intensity-duration-frequency (IDF
613) curves of satellite-based precipitation datasets in Peninsular Malaysia. *Atmospheric*
614 *Research* 248. <https://doi.org/10.1016/j.atmosres.2020.105203>

615 Pui, A., Sharma, A., Mehrotra, R., Sivakumar, B., Jeremiah, E., 2012. A comparison of alternatives
616 for daily to sub-daily rainfall disaggregation. *Journal of Hydrology* 470–471, 138–157.
617 <https://doi.org/10.1016/j.jhydrol.2012.08.041>

618 Rao, Y.R.S., Ramana, R.V., 2015. STORM WATER FLOOD MODELING IN URBAN AREAS.
619 *IJRET: International Journal of Research in Engineering and Technology* 04, 18–21.

620 Saad, S.M., Jemain, A.A., Ismail, N., 2018. Temporal rainfall disaggregation by a simple random
621 cascade model. *Jurnal Teknologi* 80, 77–85. <https://doi.org/10.11113/jt.v80.10957>

622 Shahid S., Wang X., Harun S.B., Shamsudin S.B., Ismail T., Minhans A., 2015. Climate variability
623 and changes in the major cities of Bangladesh: observations, possible impacts and
624 adaptation. *Reg Environ Change*. <https://doi.org/10.1007/s10113-015-0757-6>

625 Shawul, A. A, Chakma, S., 2020. Trend of extreme precipitation indices and analysis of long-term
626 climate variability in the Upper Awash basin, Ethiopia. *Theoretical and Applied*
627 *Climatology*. <https://doi.org/10.1007/s00704-020-03112-8>

628 Shrestha, A., Babel, M.S., Weesakul, S., Vojinovic, Z., 2017. Developing Intensity-Duration-
629 Frequency (IDF) curves under climate change uncertainty: The case of Bangkok, Thailand.
630 *Water* 9. <https://doi.org/10.3390/w9020145>

631 Sillmann, J., Thorarinsdottir, T., Keenlyside, N., Schaller, N., Alexander, L. V, Hegerl, G.,
632 Seneviratne, S.I., Vautard, R., Zhang, X., Zwiers, F.W., 2017. Understanding , modeling
633 and predicting weather and climate extremes : Challenges and opportunities. *Weather and*
634 *Climate Extremes* 18, 65–74. <https://doi.org/10.1016/j.wace.2017.10.003>

635 Solaiman, T.A., Simonovic, S.P., 2011. Development of Probability Based Intensity- Duration-
636 Frequency Curves under Climate Change. London, Canada.

637 Stephenson, A.G., Lehmann, E.A., Phatak, A., 2016. A max-stable process model for rainfall
638 extremes at different accumulation durations. *Weather and Climate Extremes* 13, 44–53.
639 <https://doi.org/10.1016/j.wace.2016.07.002>

640 Sun, Y., Wendi, D., Kim, D.E., Liang, S.Y., 2019. Deriving intensity – duration – frequency (IDF
641) curves using downscaled in situ rainfall assimilated with remote sensing data. *Geoscience
642 Letters* 6. <https://doi.org/10.1186/s40562-019-0147-x>

643 Tesfay, A., Quraishi, S., 2017. Impact of Climate Change on the Development of Rainfall
644 Intensity, Duration and Frequency Curves in Chiro and Hurso Stations of Eastern Ethiopia.
645 *Earth Sciences* 6, 97–105. <https://doi.org/10.11648/j.earth.20170605.16>

646 Waseem, M., Mani, N., Andiego, G., Usman, M., 2017. a Review of Criteria of Fit for
647 Hydrological Models. *International Research Journal of Engineering and Technology* 04,
648 1765–1772.

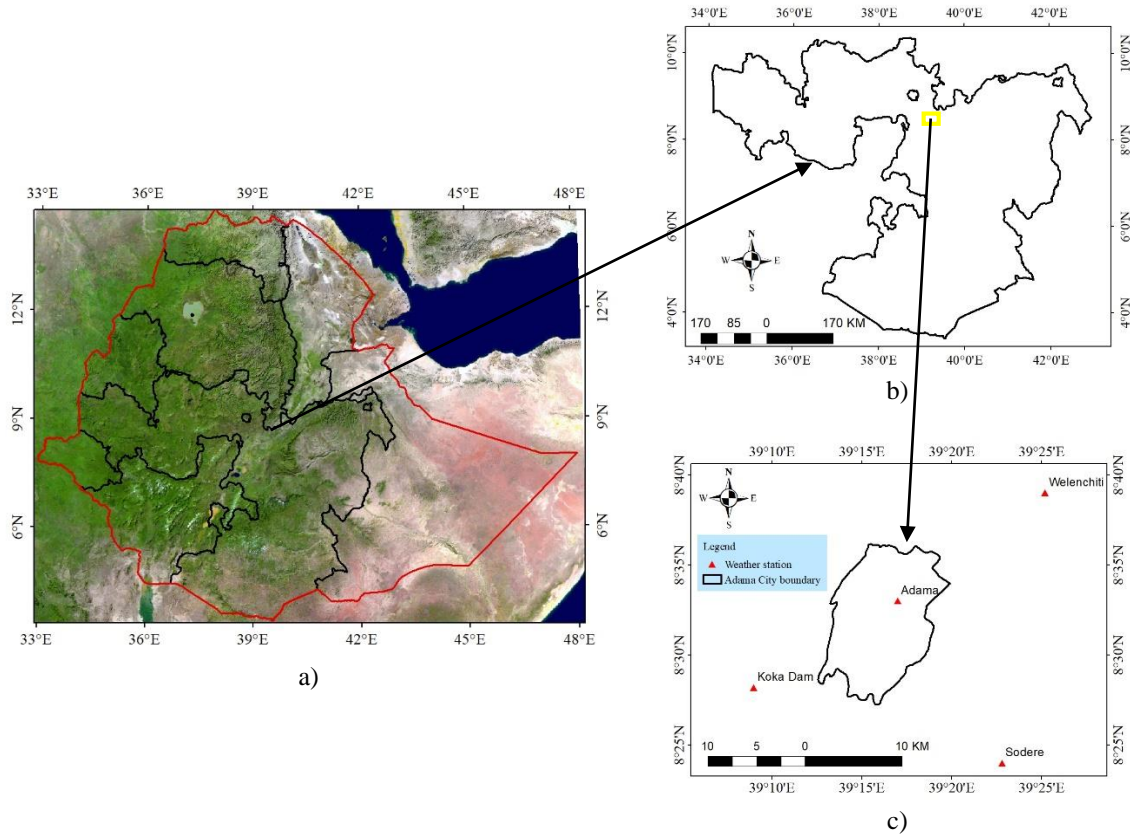
649 Yilmaz, A.G., Hossain, I., Perera, B.J.C., 2014. Effect of climate change and variability on extreme
650 rainfall intensity-frequency-duration relationships: A case study of Melbourne. *Hydrology
651 and Earth System Sciences* 18, 4065–4076. <https://doi.org/10.5194/hess-18-4065-2014>

652 Zahiri, E.-P., Bamba, I., Famien, A.M., Koffi, A.K., Ochou, A.D., 2016. Mesoscale extreme
653 rainfall events in West Africa: The cases of Niamey (Niger) and the Upper Ouémé Valley
654 (Benin). *Weather and Climate Extremes* 13, 15–34.
655 <https://doi.org/10.1016/j.wace.2016.05.001>

656 Zeder, J., Fischer, E.M., 2020. Observed extreme precipitation trends and scaling in Central
657 Europe. *Weather and Climate Extremes* 29. <https://doi.org/10.1016/j.wace.2020.100266>

658

1



2 **Fig. 1**

3

4

5

6

7

8

9

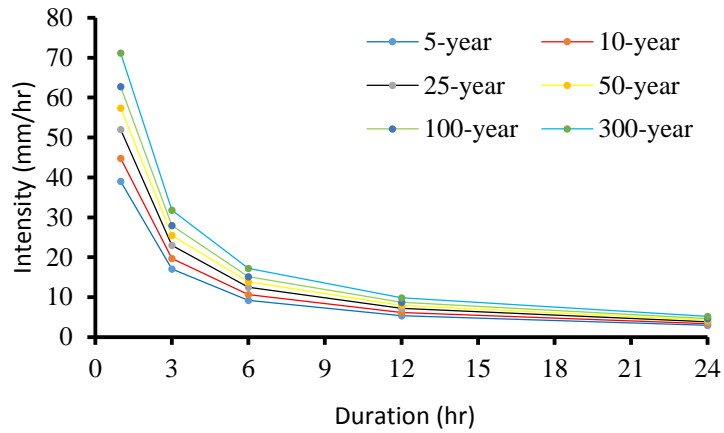
10

11

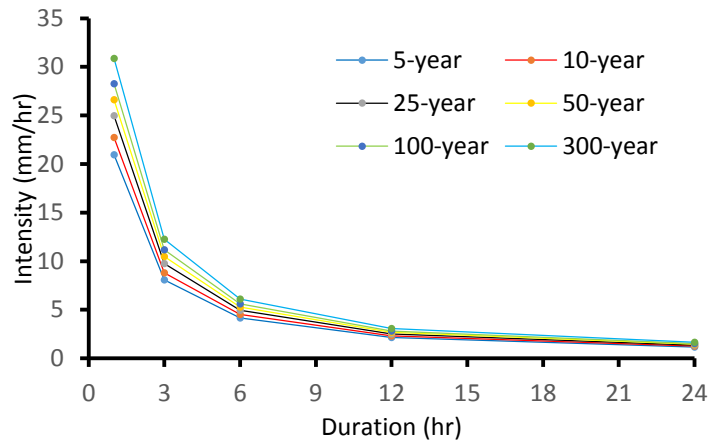
12

13

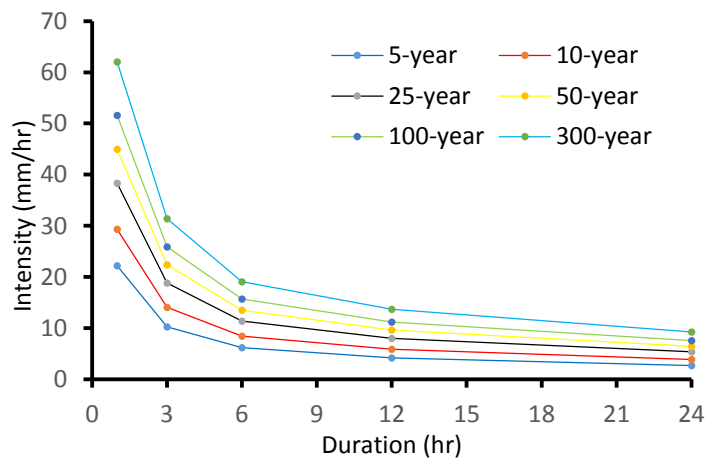
14



a) Historical (1967-2016)



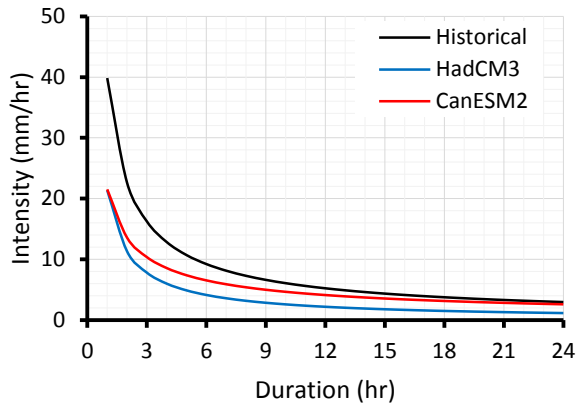
b) HadCM3 (2021-2070)



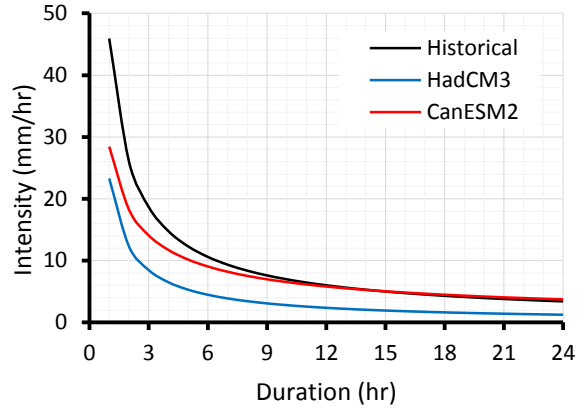
c) CanESM2 (2021-2070)

15 **Fig. 2**

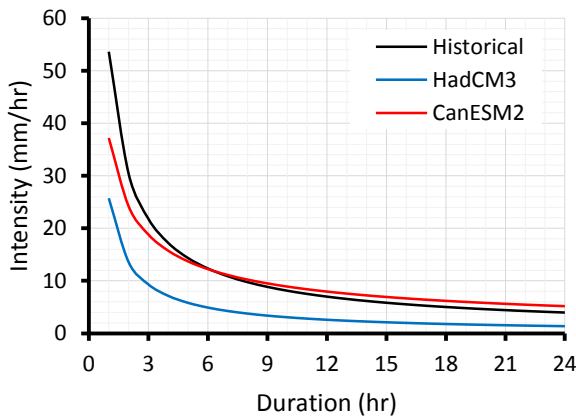
16



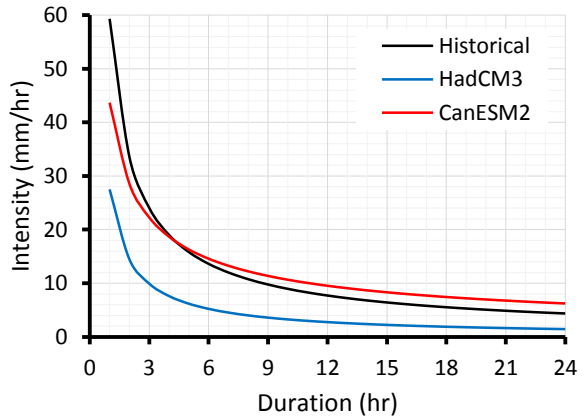
a) 5-yr



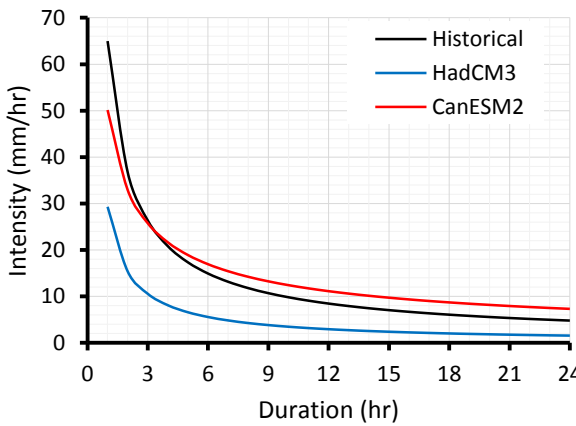
b) 10-yr



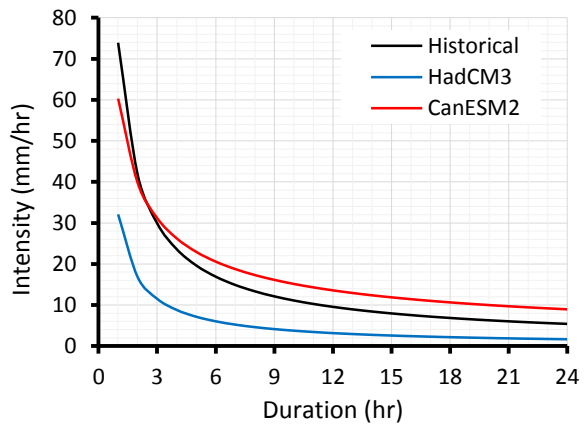
c) 25-yr



d) 50-yr



e) 100-yr



f) 300-yr

17 **Fig. 3**

1 **Table 1**

Parameter	α	κ	ϕ	$\lambda (d^{-1})$	$\mu_x (mm d^{-1})$	$v (d)$
Values	97.99	65.87	25	2.25	95.94	0.92839

2

3

4 **Table 2**

Scenarios	Storm duration				
	1-hr	3-hr	6-hr	12-hr	24-hr
Historical	1.279	0.997	1.370	0.772	0.806
HadCM3	0.510	0.754	0.577	0.371	0.356
CanESM2	1.314	1.160	1.561	1.699	1.616

5

6

7 **Table 3**

T	Historical			HadCM3			CanESM2		
	Equations	R ²	NSE	Equations	R ²	NSE	Equations	R ²	NSE
5-yr	$39.8d^{-0.816}$	0.999	0.998	$21.4d^{-0.916}$	1.000	0.968	$21.5d^{-0.665}$	0.998	0.991
10-yr	$45.9d^{-0.818}$	0.999	0.998	$23.3d^{-0.920}$	0.999	0.922	$28.4d^{-0.639}$	0.997	0.939
25-yr	$53.6d^{-0.820}$	0.999	0.997	$25.7d^{-0.925}$	0.999	0.853	$37.2d^{-0.621}$	0.997	0.820
50-yr	$59.3d^{-0.821}$	0.999	0.997	$27.5d^{-0.927}$	0.999	0.803	$43.7d^{-0.613}$	0.997	0.722
100-yr	$65.0d^{-0.822}$	0.998	0.997	$29.3d^{-0.930}$	0.999	0.757	$50.1d^{-0.607}$	0.996	0.626
300-yr	$73.9d^{-0.823}$	0.998	0.996	$32.1d^{-0.933}$	0.999	0.691	$60.3d^{-0.600}$	0.996	0.584

8

9 **Table 4**

Model parameters	Test Statistics	Historical (1967-2016)	Future (2021-2070)	
			HadCM3	CanESM2
Coefficient parameter (a)	<i>r</i>	0.863	0.864	0.864
	<i>p</i>	0.027	0.026	0.027
Exponent parameter (b)	<i>r</i>	0.757	0.796	0.683
	<i>p</i>	0.081	0.058	0.135

10

11

12 **Table 5**

T	Duration	Change in intensity (%)		T	Duration	Change in intensity (%)	
		HadCM3	CanESM2			HadCM3	CanESM2
5-yr	1	-60.3	-59.7	50-yr	1	-73.3	-30.4
	3	-70.1	-44.1		3	-83.1	-7.7
	6	-76.1	-34.0		6	-89.1	6.8
	12	-81.9	-23.7		12	-94.9	21.1
	24	-87.5	-13.3		24	-100.5	35.3
10-yr	1	-65.4	-47.0	100-yr	1	-75.7	-25.8
	3	-75.2	-28.0		3	-85.7	-2.3
	6	-81.2	-15.8		6	-91.7	12.6
	12	-87.0	-3.4		12	-97.5	27.4
	24	-92.6	9.1		24	-103.1	41.9
25-yr	1	-70.4	-36.2	300-yr	1	-78.9	-20.3
	3	-80.2	-14.7		3	-88.8	4.2
	6	-86.2	-0.9		6	-94.8	19.6
	12	-92.1	12.9		12	-100.6	34.7
	24	-97.7	26.5		24	-106.2	49.5

13